Void Geometry Driven Spin Crossover in Zeolite-Encapsulated Cobalt Tris(bipyridyl) Complex Ion

Satish Kumar Tiwary and Sukumaran Vasudevan*

Department of Inorganic and Physical Chemistry, Indian Institute of Science, Bangalore 560 012, India

Received September 5, 1997

The cobalt(II) tris(bipyridyl) complex ion encapsulated in zeolite-Y supercages exhibits a thermally driven interconversion between a low-spin and a high-spin state—a phenomenon not observed for this ion either in solid state or in solution. From a comparative study of the magnetism and optical spectroscopy of the encapsulated and unencapsulated complex ion, supported by molecular modeling, such spin behavior is shown to be intramolecular in origin. In the unencapsulated or free state, the $[Co(bipy)_3]^{2+}$ ion exhibits a marked trigonal prismatic distortion, but on encapsulation, the topology of the supercage forces it to adopt a near-octahedral geometry. An analysis using the angular overlap ligand field model with spectroscopically derived parameters shows that the geometry does indeed give rise to a low-spin ground state, and suggests a possible scenario for the spin state interconversion.

1. Introduction

The encapsulation of transition metal coordination compounds and organometallics within the voids of microporous zeolites is a convenient route to heterogenization of homogeneous catalysts.[1] Encapsulation provides a simple way of coupling the reactivity of transition metal complexes with the robustness and stereochemistry of a zeolite. The "ship-in-a-bottle" compounds,[2] which, for steric reasons, have to be assembled in situ by bringing the metal and ligand species within the voids of the zeolite, are a fascinating class of encapsulated compounds. At a simplistic level, they may be considered as inorganic analogues of natural enzymes, with the zeolite framework representing a rigid protein mantle.[3] The fundamental question is, how does the structure and reactivity of a ship-in-a-bottle species compare with those of the identical species in solution or in solid state? It is likely that the topology of the void has a profound influence on the geometry that the encapsulated complex adopts, leading in turn to appreciable changes in the electronic and magnetic properties of the complex.

One of the more dramatic changes following encapsulation, a detailed investigation of which is reported here, was observed by Mizuno and Lunsford.[4] Their electron paramagnetic resonance measurements indicated that the ship-in-a-bottle complex, cobalt(II) tris(bipyridyl) complex ion, $[Co(bipy)_3]^{2+}$, encapsulated in the supercages of zeolite-Y, exhibits a temperature-driven interconversion between a low-spin state and a high-spin state. This observation is interesting, because normally, the trigonally distorted $[Co(bipy)_3]^{2+}$ complex ion, both in solution and in solid state, retains a high-spin ground state, irrespective of the temperature or the nature of the counterion.[5]

The size of the $[Co(bipy)_3]^{2+}$ ion, ∼12 Å, makes it larger than any of the channnels and windows of the zeolite-Y structure, so it is impossible to synthesize the complex outside and then insert it into the zeolite. The complex has to be assembled within the supercage of zeolite-Y—the only cavity large enough to hold the complex. We have carried out a comparative spectroscopic and magnetic investigation of the $[Co(bipy)_3]^{2+}$ ion encapsulated in zeolite-Y and its unencapsulated state, as in the $[Co(bipy)_3](ClO_4)_2$ salt. Considerable changes, on encapsulation have been observed in the optical spectra and magnetic behavior. Both high-spin and low-spin states for the Co(II) ion have to be invoked to interpret the properties of the encapsulated complex. Our results show that the observed spin-state interconversion is intramolecular in origin.

In the unencapsulated state the $[Co(bipy)_3]^{2+}$ complex ion exhibits a trigonal prismatic distortion from octahedral symmetry. To determine the minimum-energy geometry for the complex within the supercage of zeolite-Y, a molecular mechanics (MM)[6] calculation was used. It shows that the effect of encapsulation on the $[Co(bipy)_3]^{2+}$ ion is not a simple "pressure" effect in which the complex ion is "squeezed"; the complex still has a trigonal prismatic distortion, but the geometry is close to octahedral.[7] An analysis using the angular overlap ligand field (AOLF) model,[8] with spectroscopically derived parameters, shows that this geometry does indeed give rise to a low-spin ground state for the encapsulated ion, and suggests a possible scenario for the spin state interconversion.

2. Experimental Procedures

Preparation and Characterization. $[Co(bipy)_3]^{2+}$ ion encapsulated in Zeolite-Y was prepared from Co^{2+}-exchanged zeolite-Y following the procedure of Mizuno and Lunsford,[4] who had characterized the materials and also established the stoichiometry of the encapsulated complex. Similar characterization procedures were adopted in the present work. Encapsulation was effected by heating a mixture of Co^{2+}-

(1) Balkus, K. J. Jr.; Gabrielov, A. G. *J. Inclusion Phenom. Mol. Recognit. Chem.* **1995**, *21*, 159. De Vos, D. E.; Knops-Gerrits, P. P.; *et al. J. Inclusion Phenom. Mol. Recognit. Chem.* **1995**, *21*, 185. Dutta, P. K. *J. Inclusion Phenom. Mol. Recognit. Chem.* **1995**, *21*, 215.
(2) Heron, N. *Inorg. Chem.* **1986**, *25*, 4714.
(3) Parton, R.; De Vos, D. E.; Jacobs, P. A. In *Zeolite Microporous Solids: Synthesis, Structure, and Reactivity*; E. G. Derouane, Ed.; 1992; p 555.
(4) Mizuno, K.; Lunsford, J. H. *Inorg. Chem.* **1983**, *22*, 3484.
(5) Figgis, B. N.; Gerloch, M.; Lewis, J.; Mabbs, F. E.; Webb, G. A. *J. Chem. Soc. A* **1968**, 2086.
(6) Hancock, R. D.; Martell, A. E. *Chem. Rev.* **1995**, *89*, 1875.
(7) Szalda, D. J.; Creutz, C.; Mahajan, D.; Sutin, N. *Inorg. Chem.* **1983**, *22*, 2372. (The bite angles in the unencapsulated complex $[Co(bipy)_3](ClO_4)_2$ are all different varying from 74.9 to 77.1°. Similarly, all the Co−N bond lengths are different, varying from 2.12 to 2.14 Å.)
(8) Schäffer, C. E. *Struct. Bonding* **1968**, *5*, 68.

S0020-1669(97)01147-6 CCC: $15.00
Published on Web 09/12/1998

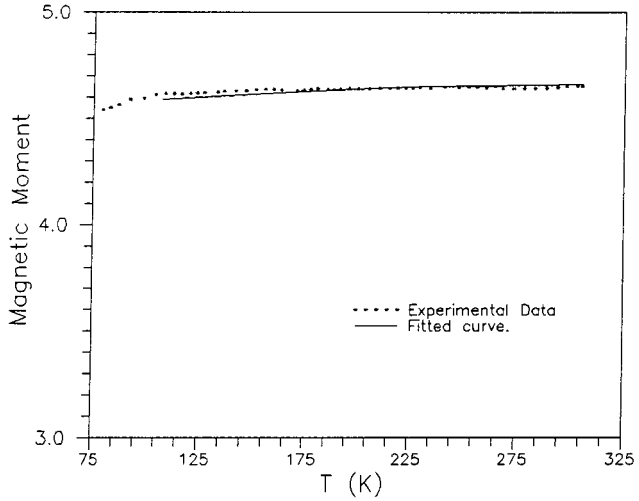

Figure 1. Magnetic moment of $[Co(bipy)_3](ClO_4)_2$ complex. The solid line is the moment calculated for $\lambda = -170$ cm^{-1} and $\Delta = -1000$ cm^{-1}.

exchanged zeolite-Y with excess bipyridyl under vacuum (10^{-3} Torr) at 473 K for 24 h. The Co^{2+}-exchanged zeolite-Y, $Co_xNa_{56-2x}Al_{56}Si_{136}O_{384}{\cdot}yH_2O$, was prepared from Na-zeolite-Y (LZY-52, Union Carbide) by ion exchange in an aqueous $Co(NO_3)_2$ solution. The cobalt loading level, x, was established by dissolving the Zeolite in HF and estimating the Co^{2+} concentration by atomic absorption spectroscopy. The loading levels, *x*, were 1, 3, and 6. The corresponding occupancies of the supercage by the encapsulated complex are 12.5, 37.5, and 75%, respectively. The encapsulated $[Co(bipy)_3]^{2+}$ samples are pale yellow and extremely moisture sensitive, changing color rapidly to pink within a few minutes on exposure to atmosphere.

The unencapsulated complex $[Co(bipy)_3](ClO_4)_2$ was synthesized by the previously reported procedure.[5] A solution of bipyridine in ethanol was added to an ethanolic solution of cobaltous chloride under an inert atmosphere. An excess of sodium perchlorate was added to the solution, which on subsequent cooling gave a yellow precipitate of $[Co(bipy)_3](ClO_4)_2$.

Magnetic Measurements. Magnetic measurements in the temperature range 50−550 K were carried out on a homemade computer-automated Faraday magnetic balance.[9] Since the encapsulated complex is extremely moisture sensitive, the samples were synthesized in small thin-walled quartz ampules (4 mm diameter, 10 mm long) following the procedure detailed above. The ampule was sealed under vacuum, and the end was fashioned into a hook so that it could be suspended from the Faraday balance. Following the magnetic susceptibility measurements, the ampule was broken and cleaned, and its diamagnetic susceptibility determined. The diamagnetic contribution of the zeolite was measured at room temperature. The paramagnetic contribution of the encapsulated complex, especially at low loading levels, is extremely small, and hence a precise determination of the diamagnetic contribution is vital for obtaining accurate values of the paramagnetic susceptibility.

Optical Spectra. The reflectance spectra were recorded on a Hitachi U3400 spectrophotometer fitted with a Hitachi integrating sphere attachment (model 151-0030) reflectance assembly. For recording the spectra of $[Co(bipy)_3]^{2+}$ in zeolite-Y, an evacuable reflectance cell was fabricated. The cell was connected to the reactor assembly via a glass tube. After the synthesis, the encapsulated complex was transferred to the cell, and the cell was isolated. The optical spectra of $[Co(bipy)_3](ClO_4)_2$ were also recorded in the reflectance mode.

A Kubelka−Munk (KM) analysis[10] was performed on the reflectance data. The KM factor, $F(R)$, is given by

$$F(\mathrm{R}) = \frac{(1-R)^2}{2R} = \frac{k}{s} \qquad (1)$$

where R is the diffuse reflectance of the sample as compared to MgO, k the molar absorption coefficient, and s the scattering coefficient of the sample.

3. Results

A. $[Co(bipy)_3](ClO_4)_2$. Magnetism. The effective magnetic moment per mole of cobalt, in the unencapsulated complex, $[Co(bipy)_3](ClO_4)_2$, is essentially temperature independent, remaining at ~4.6 μ_B down to ~90 K (Figure 1). The value of the moment is larger than the spin-only value for a high-spin d^7 ion. $[Co(bipy)_3](ClO_4)_2$ exhibits a trigonal prismatic distortion from octahedral geometry. Therefore, the data were analyzed by calculating the magnetic moment from the van Vleck susceptibility for a high-spin d^7 ion in an axially distorted ligand field corresponding to D_3 symmetry. The axial field splits the $^4T_1$ state into $^4A_2$ and a ^4E states separated by an energy Δ (Scheme 1). These states are not split further by spin−orbit coupling. The susceptibility is defined in terms of λ ($\lambda = \zeta/2S$), Δ, and A. A is defined as[11]

$$A = \frac{1.5 - c_i^2}{1 + c_i^2}$$

where c_i is the coefficient of mixing of the $^4T_1(F)$ ground state with the $^4T_1(P)$ excited state. A has a value of 1.0 in the strong-field limit and 1.5 in the weak-field limit of the ligand field theory. Analytical expressions for the first- and second-order Zeeman terms for a $^4T_1$ term in an axial field are not obtainable and had to be evaluated numerically. These were then substituted in the van Vleck equation.[11]

$$\chi = \frac{N\Sigma_i((E_i^{(1)})^2/k_BT - 2E_i^{(2)})\exp(-E_i^0/k_BT)}{\Sigma_i \exp(-E_i^0/k_BT)} \qquad (2)$$

In eq 2, $E^0{}_i$ is the energy of the ith state in the absence of magnetic field, and $E^{(1)}{}_i$ and $E^{(2)}{}_i$, are the respective first- and second-order Zeeman terms for the ith state. The calculated magnetic moment was fitted to the experimental data by a nonlinear least-squares fitting procedure allowing A, Δ, and λ to float. The best fit was obtained for $A = 1.35$, $\lambda = 170$ cm^{-1}, and $\Delta = 6\lambda$ and is shown as the solid line in Figure 1.

Optical Spectra. The optical reflectance spectrum of $[Co(bipy)_3](ClO_4)_2$ shows peaks at 11 000 and 22 100 cm^{-1} (Figure 2). The position of the peak compares well with that reported in the literature.[12]

The reflectance spectrum of $[Co(bipy)_3](ClO_4)_2$ was interpreted assuming a trigonal prismatically distorted octahedral geometry for cobalt(II). It was analyzed for a d^7 ion in a high-spin ground state in which a trigonal prismatic distortion splits the octahedral $^4T_1$ ground state into $^4A_2$ and ^4E states, separated by an energy Δ. The energies of the spin-allowed transitions were calculated using ligand field theory and considering the interelectron repulsion in terms of Raccah parameters, B and C.[13] The energies were calculated using the strong field interelectron repulsion matrixes for a d^7 ion, allowing for full interconfigurational mixing. The latter is important since an intermediate ligand field is the more appropriate for the Co^{2+} ion in a high-spin state. For complexes having D_3 or D_{3d}

(9) Tiwary, S. K. Ph.D. Thesis, Indian Institute of Science, Bangalore, India, 1996.
(10) Hecht, H. G. In *Modern Aspect of Reflectance Spectroscopy*; Wendlandt, W. W. Ed.; Plenum Press: New York, 1968.
(11) Mabbs, F. E.; Machin, D. J. *Magnetism and Transition Metal Complexes*; Chapman and Hall: London, 1973.
(12) Palmer, R. A.; Piper, T. S. *Inorg. Chem.* **1966**, *5*, 864.
(13) Griffith, J. S. *The Theory of Transition Metal Ions*; Cambridge University Press: Cambridge, 1961.

Scheme 1

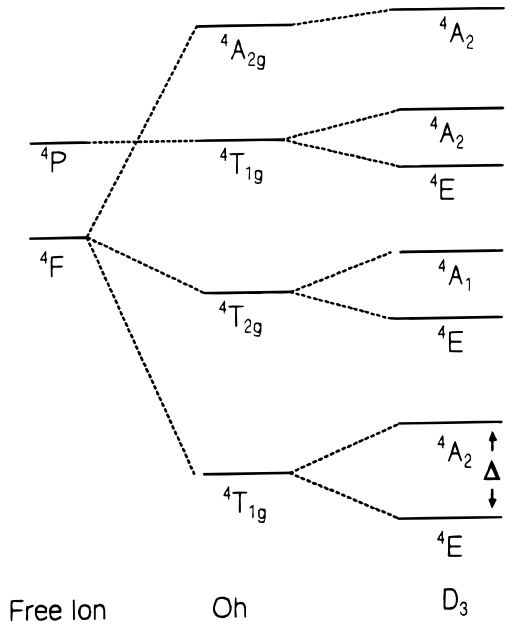

symmetry, the trigonal distortion may be treated as a perturbation on the ligand field Hamiltonian for octahedral geometry. The parameters which now describe the ligand field, in addition to Dq, are D_σ and D_τ. The latter two parameters are defined in terms of the nonvanishing matrix elements of the trigonal perturbation potential for the different strong field d orbitals which transform in the D_3 and D_{3d} representations.[14] In calculating the transition energies, the value of C was assumed to be equal to $4B$, a widely used approximation for the first-row transition metal ions.[15] The spin−orbit coupling parameter, ζ, was assumed to have the free ion value[15] of 510 cm^{-1}, and the value of Δ, the splitting in the ground state, was -1000 cm^{-1}, as obtained from fitting the magnetic data. The best agreement between the calculated and experimental transition energies was obtained for $Dq = 1205$ cm^{-1}, $D_\sigma = 100$ cm^{-1}, $D_\tau = 85$ cm^{-1}, and $B = 780$ cm^{-1}. The experimental and calculated peak positions and their assignments are given in Table 1.

B. $[Co(bipy)_3]^{2+}$ Complex Ion Encapsulated in Zeolite-Y. Optical Spectra. The optical reflectance spectrum of the encapsulated $[Co(bipy)_3]^{2+}$ complex ion, recorded in the vacuum reflectance cell, is shown in Figure 1 (a spline-fitted background has been subtracted from the spectra). The spectrum of the encapsulated complex is quite different from that of the unencapsulated $[Co(bipy)_3](ClO_4)_2$ spectra. The strong band in the near-IR at 11 300 cm^{-1} seen in the spectra of the unencapsulated complex is no longer observed in the encapsulated complex. Prominent features at 23 200, 20 800, 14 300, and 12 300 cm^{-1} may be seen.

Magnetism. The temperature variation of the magnetic moment of the encapsulated complex for different occupancies of zeolite-Y supercages is shown in Figure 3. The moment of the encapsulated complex shows a strong temperature dependence. At low temperatures, between 50 and 75 K, it remains essentially constant at 1.9 μ_B. Above 75 K, the value of the moment increases with temperature reaching 3.3 μ_B at 525 K. The slope of the μ_{eff} vs temperature is the steepest between 100 and 150 K. The value of the moment below 75 K, 1.9 μ_B, is that expected for a low-spin d^7 ion ($S = {}^1/_2$) in an octahedral field, while the value at higher temperatures is intermediate between that expected for a high-spin d^7 ion (4.2−5.2 μ_B) and its low-spin value. It may be seen that the moment as well as its temperature dependence is independent of the occupancy of the supercages.

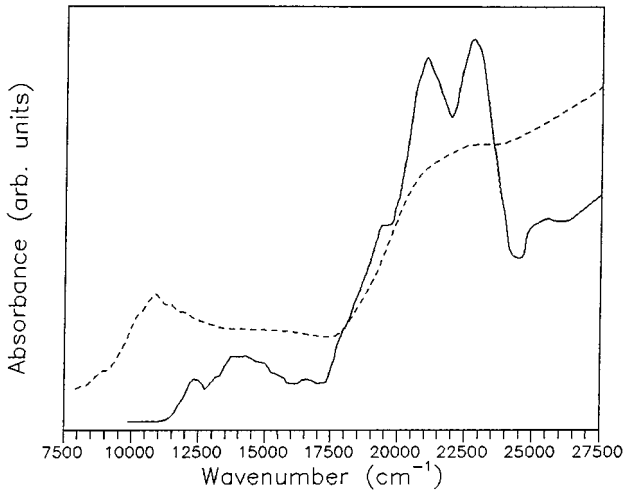

Figure 2. Optical reflectance spectra of $[Co(bipy)_3](ClO_4)_2$ (dashed line) and $[Co(bipy)_3]^{2+}$ complex ion encapsulated in zeolite-Y (solid line).

Table 1. Experimental and Calculated Peak Positions (cm^{-1}) for the Optical Spectra of $[Co(bipy)_3](ClO_4)_2$ and Their Assignments (Parent Octahedral Terms Are Given in Parentheses)

experimental	calculated	assignment
11 300	10 828	$^4E(^4T_1) \rightarrow {}^4E(^4T_2)$
	11 276	$^4E(^4T_1) \rightarrow {}^4A_1(^4T_2)$
21 275	21 231	$^4E(^4T_1) \rightarrow {}^4E(^4T_1)$
	21 680	$^4E(^4T_1) \rightarrow {}^4A_2(^4T_1)$
22 470	22 555	$^4E(^4T_1) \rightarrow {}^4A_2(^4A_2)$

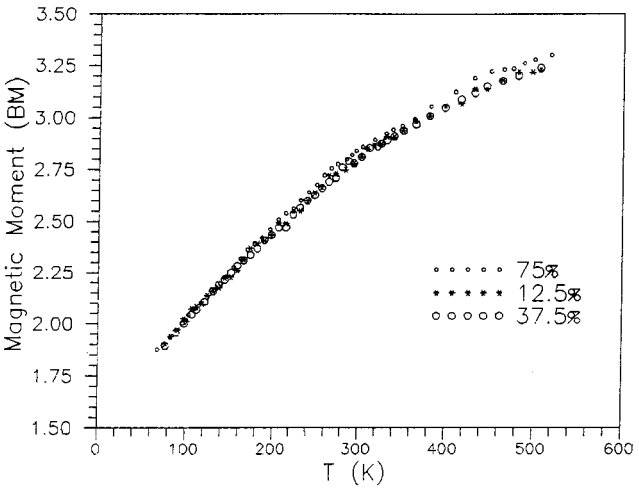

Figure 3. Magnetic moment of $[Co(bipy)_3]^{2+}$ complex ion encapsulated in Zeolite-Y for varying occupancies of the supercage. The occupancies are indicated in the figure.

4. Discussion

A comparison of Figures 1 and 3 shows that the changes in the magnetic behavior following encapsulation are quite dramatic. While the value of the moment of the unencapsulated ion remains constant at ~4.6 μ_B ($S = {}^3/_2$) over most of the temperature range, the encapsulated complex shows a gradual increase in the value of its moment, a behavior typical of spin-

(14) Ballhausen, C. J. *Introduction to Ligand Field Theory*; McGraw-Hill: 1962.
(15) Lever, A. B. P. *Inorganic Electronic Spectroscopy*, 2nd ed.; Elsevier: 1984.

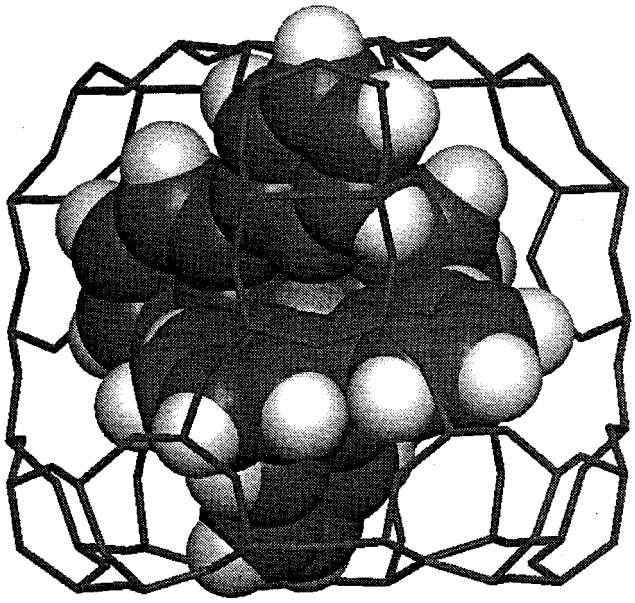

Figure 4. Molecular graphic representation of $[Co(bipy)_3]^{2+}$ complex ion having the free state geometry, encapsulated in zeolite-Y. The figure is of the orientation having minimum interaction energy with the walls of the supercage.

state interconversion. The optical reflectance spectrum (Figure 2) also shows considerable change on encapsulation and may be interpreted as arising due to transitions from both low-spin and high-spin ground states of a Co^{2+} ion. The questions that arise from these observations are, why is the spin state of the encapsulated complex different from that in its unencapsulated state, and what is the origin of its temperature dependence? The fact that the moment of the encapsulated complex is independent of the occupancy of the supercages suggests that cooperative interactions between $[Co(bipy)_3]^{2+}$ units, similar to those found in the optical behavior of encapsulated $[Ru(bipy)_3]^{2+}$,[16] are unlikely to be important. If cooperative effects were important, then a dilution effect should be manifest either as a change in the value of the moment as a function of cage occupancy or in its temperature variation, similar to that observed in systems undergoing a spin-state transition, e.g. when the crystals of $Fe(phen)_2(NCS)_2$ (phen = 1,10 phenanthroline) are diluted with any of the following metal ions: Mn^{2+}, Co^{2+}, Ni^{2+}, or Zn^{2+}.[17]

The change in the spin state on encapsulation as well as the variation of the moment with temperature are intramolecular in origin, probably arising as a consequence of the fact that on encapsulation, $[Co(bipy)_3]^{2+}$ adopts a geometry different from that found in the unencapsulated state. This was evident from a molecular graphics analysis[18] which indicated that it is impossible to fit the $[Co(bipy)_3]^{2+}$ ion having the same trigonally distorted geometry of the unencapsulated state without causing it to "bump" into the walls of the supercage (Figure 4). It was also obvious from the analysis that if the bumps were to be avoided by shortening the Co−N bonds, a considerable reduction (2.13 → 1.8 Å: 15%) would be needed, which would be energetically unfavorable. It is more likely that on encapsulation, the $[Co(bipy)_3]^{2+}$ ion adopts a geometry different from that in its unencapsulated state.

Molecular Mechanics. Molecular mechanics was used to determine the minimum-energy geometry of the encapsulated complex. The potential energy for the $[Co(bipy)_3]^{2+}$ ions having different geometries within the supercages of zeolite-Y was calculated. The total potential energy of an encapsulated complex is a sum of two parts:

(i) An internal energy which is dependent on the geometry of the complex. This for $[Co(bipy)_3]^{2+}$ may be defined in terms of the bite and twist angles, α and ϕ respectively, and the Co−N equilibrium bond length, r_{Co-N}.[19] (The bite angle is the angle that the two ligating N-atoms of the bipyridyl ligand make at the central cobalt atom; the twist angle is the angle the two triangular faces of the complex along the principal C_3 axis make with each other.) In the present calculations, the bipyridyl ligand was considered as a rigid moiety.

(ii) The energy of interaction of the encapsulated complex with the walls of the zeolite host, which depends on the position and orientation of the complex inside the host.

The geometry adopted by the complex on encapsulation was obtained by minimizing the total potential energy with respect to the geometrical parameters of the complex as well as its position and orientation within the supercage.

The internal energy of the complex was calculated as a function of bite and twist angles using the universal force field (UFF)[20] with the parameters chosen in such a way that the model predicted the trigonal prismatically distorted geometry of the complex $[Co(bipy)_3]^{2+}$ ion in $[Co(bipy)_3](ClO_4)_2$ to be the minimum-energy geometry. The internal energy was calculated as a function of the bite and twist angles for fixed r_{Co-N} values. The values of r_{Co-N} used for the calculation were 2.13 Å, similar to that in the high-spin free state, and 2.03 Å, which was considered as representative of a low-spin Co^{II}−N bond length.

The energy of interaction of the $[Co(bipy)_3]^{2+}$ ions with the walls of the supercage of zeolite-Y was calculated using the Lennard-Jones 6-12 potential for van der Waals interactions. Electrostatic interactions were ignored. The interaction energy was minimized as a function of the orientation and the position of the center of gravity of the complex using the Monte Carlo energy minimization scheme of the Biosym Catalysis−Solids Docking software package.[18]

The total potential energy of the encapsulated complex as a function of its bite and twist angles for $r_{Co-N} = 2.13$ Å is shown in Figure 5. In this figure, for each geometry (i.e., bite and twist angles), the interaction energy of the complex with the walls of the supercage has been minimized. The minimum energy occurs for a geometry with bite = 80° and twist = 55°. These values may be contrasted with the values of bite = 75° and twist = 40° observed for the complex in its free state. The geometry of the encapsulated complex is thus much closer to that of a regular octahedron (bite = 90°, twist = 60°). Molecular graphics (Figure 6) shows why this is so; this geometry allows the complex to be positioned in such a way that large sections of the bipyridyl groups are accommodated within the windows of the supercage which are tetrahedrally disposed. The closer the geometry of the complex is to that of a regular octahedron, the easier it is to accommodate the bulky ligands within the windows, and hence lower the interaction energy. The results for $r_{Co-N} = 2.03$ Å are shown in Figure 7 and show that the minimum energy geometry (bite = 85°, twist = 55°) is now still closer to that of a regular octahedron.

The accuracy of the energy values as obtained from a MM calculation, obviously, depends on the quality of the force field

(16) Turbeville, W.; Robins, D. S.; Dutta, P. K. *J. Phys. Chem.* **1992**, *96*, 5024.
(17) Ganguli, P.; Gutlich, P.; Müller, E. W. *Inorg. Chem.* **1982**, *21*, 3429.
(18) *Biosym Catalysis*, version R4.0; Biosym Technologies: San Diego, CA, 1993.
(19) Kepert, D. L. *Inorganic Stereochemistry*; Springer-Verlag: Berlin, 1982.
(20) Rappe, A. K.; Colwell, K. S.; Casewit, C. J. *Inorg. Chem.* **1993**, *32*, 3438; Rappe, A. K.; Casewit, C. J.; Colwell, K. S.; Goddard, W. A., III; Skiff, W. M. *J. Am. Chem. Soc.* **1992**, *114*, 10024.

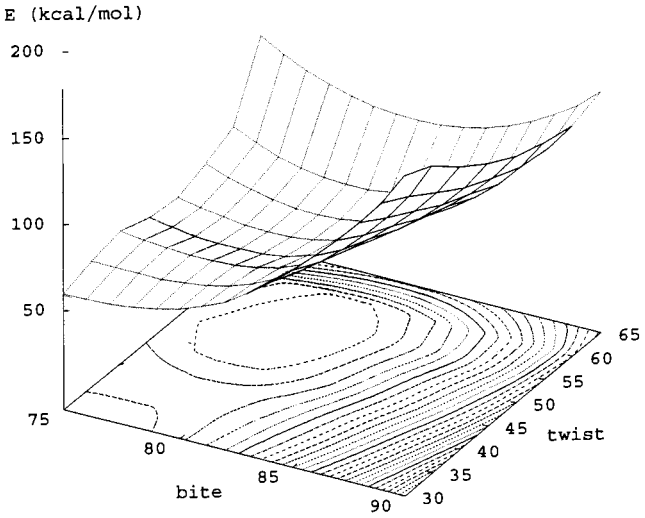

Figure 5. Total potential energy as a function of bite and twist angles for an encapsulated $[Co(bipy)_3]^{2+}$ complex ion (r_{CO-N} = 2.13 Å).

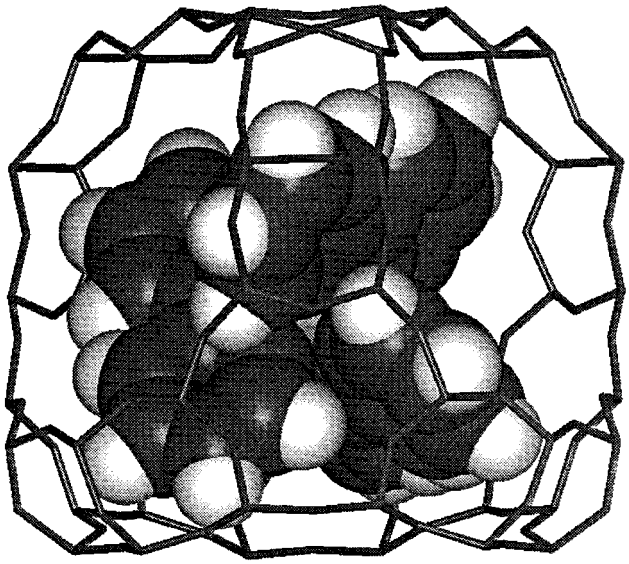

Figure 6. Molecular graphic representation of $[Co(bipy)_3]^{2+}$ complex ion, having the minimum energy geometry (bite = 80°, twist = 55°), encapsulated in zeolite-Y. The figure is of the orientation having minimum interaction energy with the walls of the supercage.

used. In the present exercise, no claim is made on the absolute values of the energies, considering the approximate nature of the force field used. The calculations are, however, representative, and are thus able to predict the trend in energy versus geometrical parameters of the encapsulated complex.

The MM calculations show that the geometry of the encapsulated complex is different from that of the free state complex. The geometry adopted is the resultant of two competing factors: the host−guest interactions which favor an octahedral geometry (bite = 90°, twist = 60°) and the internal energy which prefers a D_3 geometry (bite = 75°, twist = 40°). On encapsulation, $[Co(bipy)_3]^{2+}$ adopts a more octahedral-like structure, with the values of bite and twist depending on the value of r_{Co-N}. It is interesting to note that both the twist and bite angles are affected by encapsulation. The twist changes from 40 to 55°, whereas the bite changes from 75 to 80−85°. A change in only the bite angle would correspond to a pressure effect. The point group symmetry of the encapsulated complex is still D_3, but encapsulation has brought the symmetry closer to D_{3d} (twist = 60°).

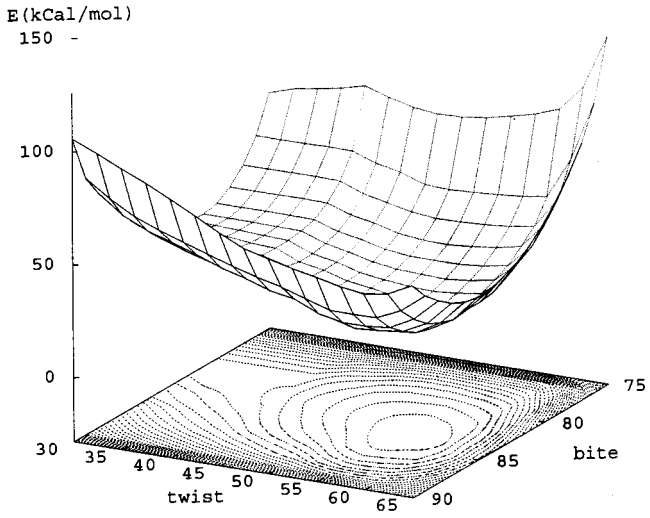

Figure 7. Total potential energy as a function of bite and twist angles for an encapsulated $[Co(bipy)_3]^{2+}$ complex ion (r_{CO-N} = 2.03 Å).

Molecular Term Energies. To determine how the changed geometry of CobpZY would affect the electronic properties, the molecular term energies for $[Co(bipy)_3]^{2+}$ were calculated along the bite (α) and twist (ϕ) coordinates. The angular overlap ligand field (AOLF)[8] model was used to construct bases of *d*-type MO's for various values of α and ϕ. Slater determinants were constructed in these bases and linear combination of the determinants diagonal under $\hat{S}^2$ used to generate a matrix for the electron repulsion operator, e^2/r, for each distinct geometry. Diagonalization of this matrix yields the term energies.[21] The d−d electron repulsion are described in terms of the spectroscopically derived Raccah interelectron repulsion parameters, *B* and *C*, which were assumed to be geometry independent.

For a trigonally distorted complex, having D_3 symmetry, the t_2 orbital splits into an e and an a_2 orbital, either of which could be lower in energy, depending on the signs of D_σ and D_τ. The parameters *Dq*, D_σ, and D_τ are related to the AOLF parameters e_σ and e_π by the following relations:[22]

$$Dq = \frac{3\sqrt{2}}{8}\sin^3\theta\cos\theta\left[\frac{9}{5}e_\sigma - \frac{12}{5}e_\pi\right] \quad (3)$$

$$D_\sigma = -\frac{3}{7}(3\cos^2\theta - 1)[e_\sigma + e_\pi] \quad (4)$$

and

$$D_\tau = -\left[\frac{1}{28}(35\cos^4\theta - 30\cos^2\theta + 3) + \frac{\sqrt{2}}{4}\sin^3\theta\cos\theta\right] \times \left[\frac{9}{5}e_\sigma - \frac{12}{5}e_\pi\right] \quad (5)$$

The angle θ is defined by the following relation

$$\sin^2\theta = \frac{1+\cos\alpha}{1+\cos\phi}$$

The possible ground-state configurations for d^7, according to the above splitting scenario, are $a_2^2e_t^4e_e^1$, $a_2^1e_t^4e_e^2$, and $a_2^2e_t^3e_e^2$. The first configuration gives rise to a low-spin ground state, whereas the other two produce high-spin ground states.

(21) Purcell, K. F. *J. Am. Chem. Soc.* **1979**, *101*, 5147.
(22) König, E.; Kremer, S. *Ligand Field Energy Diagrams*; Plenum Press: New York, 1977.

The ground terms corresponding to the three states are ^2E, $^4A_2$, and ^4E, respectively.

In calculating the AOLF energies for $[Co(bipy)_3]^{2+}$, π interactions have been neglected. The reason for this is that in the $[Co(bipy)_3]^{2+}$ complex, the value of the length of the C−C bond which joins the two pyridine units (1.49 Å) is equal to that observed in the free molecule, implying that the π interactions are very small. The pyridine group of ligands are weak π acceptors,[15] with e_π values usually within 50−100 cm^{-1}. The values of e_σ for the HS and LS ground states were obtained from their respective optically derived *Dq* values. Using these values of e_σ, the trigonal crystal field parameters D_σ and D_τ were evaluated for various values of the bite (α) and twist (ϕ) angles and hence the crystal field energies, as a function of α and ϕ, for the various configurations transforming as $^4A_2$, ^4E, and ^2E.

The electron repulsion energies associated with these configurations were calculated by evaluating the two-electron repulsion integrals in terms of Raccah *B* and *C* parameters.[13] Interconfigurational mixing was included by setting up the appropriate matrix elements for each term. Only those configurations which differ from the lowest energy configuration by at most 10*Dq* were included. The complete energy matrix for each term was obtained by adding the appropriate ligand field energy, as calculated from the AOLF model, to the diagonal elements for the various configurations. Diagonalization of these matrixes gave the molecular term energies in terms of *Dq*, *B*, and *C*.

The values of the ligand field parameters were obtained from an analysis of the optical spectra of the encapsulated complex. The molecular mechanics calculations of the previous section have shown that the $[Co(bipy)_3]^{2+}$ complex ion adopts a near-octahedral geometry on encapsulation. Though the geometry of the complex is still D_3, the deviation from the octahedral geometry is small, and consequently, the splitting of the octahedral levels due to the small trigonal field is unlikely to be seen because of the intrinsic line widths of the transitions. The optical spectra of the encapsulated complex was, therefore, interpreted assuming an octahedral geometry for the $[Co(bipy)_3]^{2+}$ ion and ignoring the small deviation from octahedral symmetry. The magnetic data had indicated that the encapsulated species at room temperature consists of both high-spin (HS) and low-spin (LS) states in equilibrium. Consequently, it may be anticipated that the features from both high-spin and low-spin states would be present in the optical spectra. Ignoring the slight trigonal distortion, the ground states would then be $^4T_1$ for the HS and ^2E for the LS state. Tentative assignments based on the spin-allowed transitions of both the ground states are 12 345 cm^{-1}, $^4T_1 \rightarrow {}^4T_2$; 14 285 cm^{-1}, $^2E \rightarrow {}^2T_1$; 20 835 cm^{-1}, $^2E \rightarrow {}^2T_1$; and 23 255 cm^{-1}, $^4T_1 \rightarrow {}^4T_1$.

Both HS and LS features were analyzed in the strong-field limit of ligand field theory allowing for full interconfigurational mixing. The relation $C = 4B$ was assumed, as before. The best agreement, using a least-squares fit algorithm, was obtained for $Dq = 1425$ cm^{-1} and $B = 780$ cm^{-1} for the HS state and $Dq = 1605$ cm^{-1} and $B = 780$ cm^{-1} for the LS state. The experimental and calculated peak positions, along with their assignments, are given in Table 2. The calculated positions of the spin-forbidden bands have been marked on Figure 8. It may be seen that some of the weak features in the optical spectra, e.g. at 13 600, 15 300, 19 700, 25 510 cm^{-1} etc., coincide with the values of the calculated transition energies. Allowing for full interconfigurational mixing, and assuming $C = 4B$, a spin crossover situation arises at $Dq = 1.94B$, which for $B = 780$ cm^{-1} occurs at 1515 cm^{-1}. It is interesting to note that this is the arithmetic mean of the *Dq* values obtained for the LS (1605 cm^{-1}) and HS (1425 cm^{-1}) states from the analysis of the optical spectra.

Table 2. Experimental and Calculated Peak Positions (cm^{-1}) for the Optical Spectra of $[Co(bipy)_3]^{2+}$ Encapsulated in Zeolite-Y

experimental	calculated	assignment
12 345	12 894	$^4T_1 \rightarrow {}^4T_2$
13 600	13 464	$^4T_1 \rightarrow {}^2T_1$
	13 499	$^4T_1 \rightarrow {}^2T_2$
14 285	14 280	$^2E \rightarrow {}^2T_1$
	14 335	$^2E \rightarrow {}^2T_2$
15 300	15 511	$^2E \rightarrow {}^4T_2$
19 700	19 705	$^4T_1 \rightarrow {}^2T_1$
20 835	20 820	$^2E \rightarrow {}^2T_2$
23 255	23 240	$^4T_1 \rightarrow {}^4T_1$
25 510	25 375	$^4T_1 \rightarrow {}^2A_1$
	25 784	$^2E \rightarrow {}^4T_1$

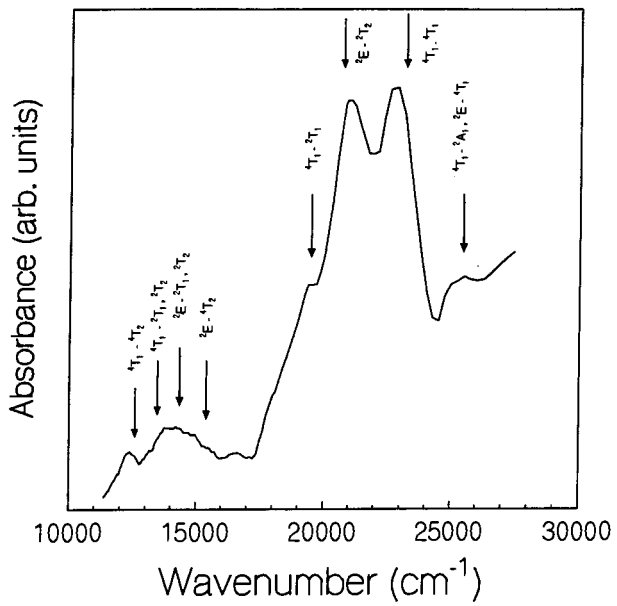

Figure 8. Optical reflectance spectra of $[Co(bipy)_3]^{2+}$ complex ion encapsulated in zeolite-Y. The calculated positions of the optical bands and assignments are indicated.

The energies of the $^4A_2$, ^4E, and ^2E terms, as a function of α and ϕ, were calculated for $Dq = 1605$ cm^{-1}, $B = 780$ cm^{-1}, and $C = 4B$. Calculation for $Dq = 1425$ cm^{-1} does not result in any significant difference. By combining the data, the ground state, the term with minimum energy, for varying values of the bite and twist angles was obtained and is shown in Figure 9, for $Dq = 1605$ cm^{-1}. The figure clearly shows how encapsulation brings about a change in the spin-state of the complex. Starting from the free state geometry (bite = 75°, twist = 40°), which has a high-spin ^4E ground state, the low spin ^2E state is stabilized as the bite and twist approach the values for a regular octahedron. Encapsulation of $[Co(bipy)_3]^{2+}$ complex in the supercage of zeolite-Y forces it to adopt a more octahedral-like geometry. As may be seen from Figure 9, this would drive it toward a low-spin ground state. In the region where the MM calculation predicts the minimum energy for the encapsulated complex (bite = 80−85°, twist = 55°), the low-spin ^2E and the high-spin $^4A_2$ states are comparable in energy. A minor excursion along the bite coordinate with twist remaining essentially constant at 55° would cause an intersystem crossing. Accordingly, we visualize the spin-state interconversion in encapsulated $[Co(bipy)_3]^{2+}$ as involving an equilibrium between

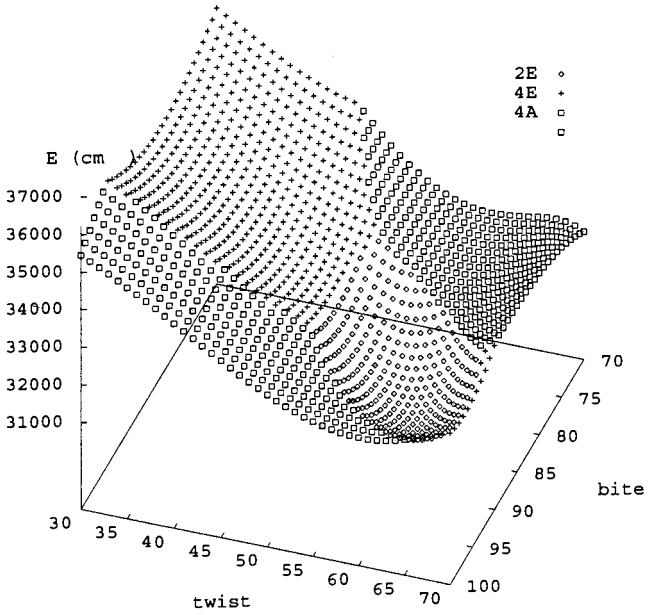

Figure 9. Molecular ground-state term and its energy for the $[Co(bipy)_3]^{2+}$ complex ion as a function of the bite and twist angles.

low-spin and high-spin isomers having ^2E and $^4A_2$ terms as their respective ground states.

Magnetism. The magnetic data of the encapsulated $[Co(bipy)_3]^{2+}$ ion were analyzed by considering HS and LS isomers in thermal equilibrium. The geometries of both isomers deviate from a perfect octahedron, but the magnitudes of the deviations, as defined by the bite and twist angles, are different for the two and consequently the ground electronic states are different. The equilibrium constant, K, can be evaluated from the experimental magnetic moment, μ_{exp}, by the following equation[11]

$$K = \frac{\mu_{exp}^2 - \mu_L^2}{\mu_H^2 - \mu_{exp}^2} \tag{6}$$

where μ_H and μ_L are the magnetic moments of the HS and LS isomers, respectively.

The equilibrium constant, K, was estimated by assuming that, at low temperatures, the equilibrium involves only the ground state of the HS and LS isomers and that excited states of neither isomer are thermally accessible. The moment associated with the ^2E ground state of the low-spin isomer, $\mu_{^2E}$, is given by

$$\mu_{^2E} = \left[3\left(1 - \frac{2\lambda}{10Dq}\right)^2 + \frac{12k_BT}{10Dq}\right]^{1/2} \tag{7}$$

where $\lambda = -510$ cm^{-1} and $Dq = 1605$ cm^{-1}, while the moment associated with the $^4A_2$ ground state of the high-spin isomer given by

$$\mu_{^4A_2} = \mu_{so}\left[1 - \frac{4\lambda}{10Dq}\right] \tag{8}$$

where μ_{so} is the spin-only magnetic moment, $\lambda = 170$ cm^{-1}, and $Dq = 1425$ cm^{-1}. Substituting the values of $\mu_{^2E}$ and $\mu_{^4A_2}$ for μ_L and μ_H, respectively, in eq 6, the equilibrium constant, K, can be evaluated. The equilibrium constant between spin isomers is given by

$$\left[\frac{d \ln K}{dT}\right]_T = \frac{\Delta G^\circ}{RT^2} \tag{9}$$

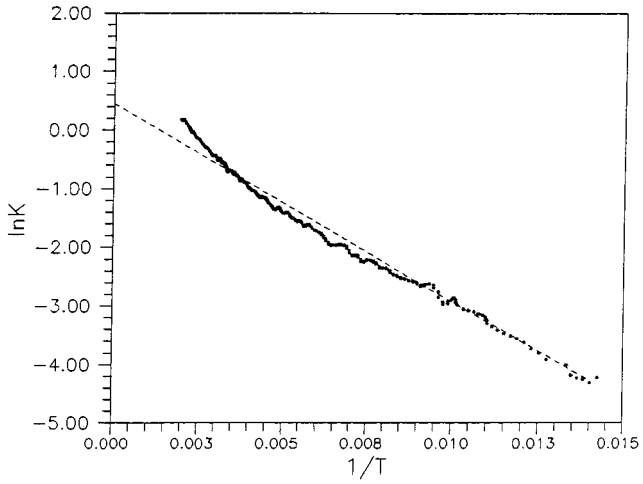

Figure 10. Calculated equilibrium constant (eqs 6−8) as a function of inverse temperature. The dashed line is the Arrhenius fit for $T <$ 120 K.

where ΔG° is the difference in the Gibbs free energy. At constant P and V,

$$\ln K = \frac{\Delta E_{HS-LS}}{RT} + \frac{\Delta S}{R} \tag{10}$$

where ΔE_{HS-LS} is the difference in molecular energies between the low- and high-spin isomers, and ΔS is the difference in entropies. Figure 10 shows the plot of ln K vs $1/T$. It is linear at low temperatures with slope ΔE_{HS-LS} of 240 cm^{-1} and a positive intercept, $\Delta S/R$ of 0.45. Since the degeneracies of the ^2E and $^4A_2$ states are identical, ΔS would have only vibrational contributions. At higher temperatures, the ln K vs $1/T$ plot is nonlinear since the excited states of the spin isomers can no longer be ignored.

In fitting the magnetic data over the entire temperature range, the energies of the excited states of the LS and HS isomers are required. This can be calculated from the AOLF model, provided the geometries of the two spin isomers are known. Since the MM geometries are only approximate, a representative calculation was carried out assuming that the twist angle for both the isomers was 55°, and that the bite coordinates were equidistant from the crossover point. For a twist of 55°, the spin crossover, as evaluated from the AOLF model, occurs at 83°, so that the bite angles for the HS and LS isomers are $83 + \Delta\alpha$ and $83 - \Delta\alpha$, respectively. The magnetic moments of the LS and HS isomers were calculated using the van Vleck's equation (eq 2). The energies of the terms for various values of $\Delta\alpha$ were obtained from AOLF molecular term energy calculations using $Dq = 1605$ cm^{-1} and $B = 780$ cm^{-1} for the LS state, $Dq = 1425$ cm^{-1} and $B = 780$ cm^{-1} for the HS state, and assuming $C = 4B$ for both the cases.

For each value of $\Delta\alpha$, the total magnetic moment was calculated considering the two spin isomers to be in equilibrium. In constructing the partition function, Q, for the above equilibrium process, it is assumed that the vibrational contribution is temperature independent, and is equal to the value of $\Delta S/R$, 0.45, as obtained from the Y intercept in Figure 10. The total moment of the encapsulated complex is given by

$$\mu^2_{\text{total}}(\Delta\alpha) = \frac{\mu^2_{\text{LS}(83+\Delta\alpha)} + \mu^2_{\text{HS}(83-\Delta\alpha)}\exp(\ln(Q_{\text{HS}}/Q_{\text{LS}}) - (\Delta E_{\text{LS-HS}}/kT))}{1 + \exp(\ln(Q_{\text{HS}}/Q_{\text{LS}}) - (\Delta E_{\text{LS-HS}}/kT))} \quad (11)$$

where $\Delta E_{\text{LS-HS}} = 240\ \text{cm}^{-1}$.

The above expression was fitted to the experimental magnetic moment by allowing $\Delta\alpha$, the only variable in eq 11, to float. For a twist of 55°, the best fit was obtained for $\Delta\alpha = 3°$. The experimental and fitted moments as a function of temperature are plotted in Figure 11. The energy diagram corresponding to the bite angles which gave the best fit to the magnetic data is shown in Scheme 2.

It is possible to fit the magnetic data of Figure 3 for different values of the twist angle varying from 53 to 57°, the corresponding bite angle at which the crossover occurs changes only marginally from 82.5 to 83.5°. The value of $\Delta\alpha$ required to obtain a good fit is roughly the same, $\Delta\alpha = 3-4°$.

It may be reemphasized that the fit shown in Figure 11 is for a representative value of twist angle, the intention being to illustrate that the spin crossover scenario described in the previous sections can adequately explain the magnetic behavior of $[Co(bipy)_3]^{2+}$ encapsulated in zeolite-Y.

5. Conclusions

We have carried out a comparative spectroscopic and magnetic investigation of the $[Co(bipy)_3]^{2+}$ complex ion encapsulated in zeolite-Y and in the unencapsulated state as in $[Co(bipy)_3](ClO_4)_2$(l). The changes in magnetic behavior following encapsulation are quite dramatic. While the value of the moment of the *unencapsulated* ion remains constant at ~4.6 μ_B ($S = {}^3/_2$) over most of the temperature range, that of the *encapsulated* complex shows a gradual increase from 1.9 μ_B ($S = {}^1/_2$) at low temperatures to a value intermediate between the HS ($S = {}^3/_2$) and LS ($S = {}^1/_2$) values at higher temperatures. The moment and its temperature dependence are independent of the occupancy of the supercage, suggesting that the mechanism of the spin-state interconversion is intramolecular in nature. The optical reflectance spectra of the encapsulated complex shows features due to transitions from both the HS and LS ground states of a Co^{2+} ion.

A molecular graphic analysis indicated that it is impossible to fit the $[Co(bipy)_3]^{2+}$ ion having the same trigonally distorted geometry of the "free" state, without causing it to bump into the walls of the supercage. We used a molecular mechanics calculation to determine the minimum energy geometry that the $[Co(bipy)_3]^{2+}$ ion would adopt on encapsulation. According to the calculations, the minimum energy structure is one in which the complex adopts a near-octahedral geometry. This allows the complex to be oriented in such a way that large sections of the bipyridyl groups are accommodated within the windows of the supercages.

To determine how the changed geometry of the encapsulated complex would affect the electronic states, the molecular term energies for the Co^{2+} ion in $[Co(bipy)_3]^{2+}$ was calculated for varying values of the bite and twist using the AOLF model with the values of the crystal field splitting parameter, *Dq*, and the Raccah interelectron repulsion parameters, *B* and *C*, derived from the optical spectra. These values are $Dq = 1425\ \text{cm}^{-1}$ and $B = 780\ \text{cm}^{-1}$ for the HS isomer, and $Dq = 1605\ \text{cm}^{-1}$ and $B = 780\ \text{cm}^{-1}$ for the LS isomer. $C = 4B$ was assumed. The AOLF calculations show that in the region where the MM calculations predict the minimum energy for the encapsulated complex, a low-spin ^2E and a high-spin $^4A_2$ states have comparable energy. A minor excursion along the bite coordinate would cause an intersystem crossing. Accordingly, the spin-state interconversion may be visualized as involving a thermal equilibrium between LS and HS isomers having ^2E and $^4A_2$ as their respective ground states. At low temperatures, the equilibrium constant for this process shows an Arrhenius behavior with $\Delta E_{\text{LS-HS}} = 240\ \text{cm}^{-1}$.

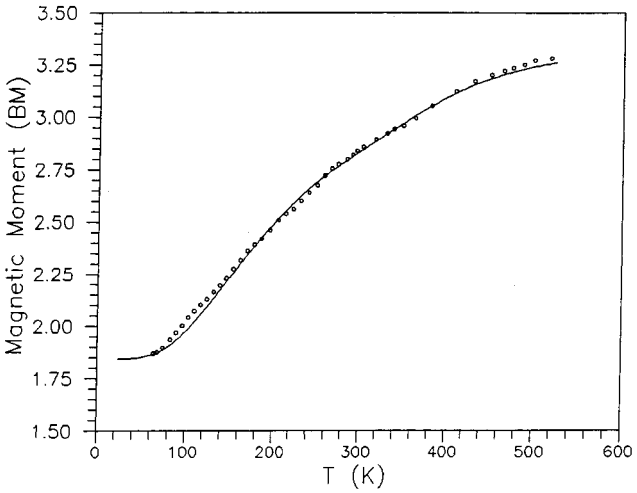

Figure 11. Comparison of the experimental and fitted magnetic moments of $[Co(bipy)_3]^{2+}$ complex ion encapsulated in zeolite-Y. The solid line is the best fit obtained for $\Delta\alpha = 3°$.

Scheme 2

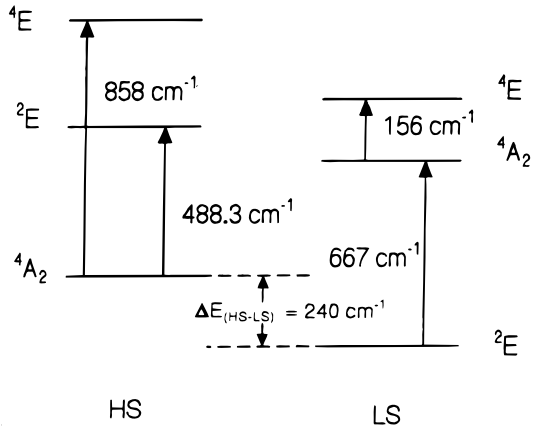

In conclusion, the present study highlights the influence of the topology of the supercage on the geometrical disposition of ligands around a metal ion in an encapsulated organometallic or coordination complex. In the case of cobalt(II) tris(bipyridyl) complex ion, the effect of encapsulation is to partially undo the trigonal distortion found in the unencapsulated ion. This change in geometry in turn leads to a change in the spin state of the cobalt ion. We believe that these observations would hold good for a variety of metal complexes and organometallics encapsulated in microporous solids and that similar effects could be observed for properties other than magnetic. Since a wide variety of microporous solids with voids of different sizes and geometries are known, encapsulation points to a number of possibilities for the exploitation of the subtle interplay between structure and properties in inorganic complexes.

Acknowledgment. The help of Mr. N. Murugapiran in synthesizing the compounds is acknowledged.

IC9711473